Mechanics of neutrophil phagocytosis: behavior of the cortical tension

Marc Herant*, Volkmar Heinrich and Micah Dembo

Biomedical Engineering Department, Boston University, 44 Cummington Street, Boston, MA 02215, USA

*Author for correspondence (e-mail: herantm@bu.edu)

Accepted 20 January 2005
Journal of Cell Science 118, 1789-1797 Published by The Company of Biologists 2005
doi:10.1242/jcs.02275

Summary

The mechanical implementation of phagocytosis requires a well-coordinated deployment of cytoplasm and membrane during the creation of a phagosome. We follow the time course of this process in initially round passive neutrophils presented with antibody-coated beads of radii 1.1 to 5.5 μm. In particular, we monitor the cortical tension as the apparent cellular surface area increases due to cell-driven deformations induced by phagocytosis. The behavior of the tension is then compared with conditions of similar area expansion caused by externally imposed deformations during cell aspiration into a micropipette. Whereas the resting tension remains low for an area expansion of up to only 30% during aspiration, it remains low even after an area expansion of up to 80% in phagocytosis. This is probably the result of membrane insertion from inner stores by exocytosis. We further find that the onset of viscous tension, proportional to the rate of area expansion and caused by the unfurling of plasma membrane wrinkles, is significantly delayed in phagocytosis compared with aspiration. We propose that this is the result of phagocytosis-triggered enzymatic activity that releases spare plasma membrane normally sequestered by velcro-like bonds in a reservoir of surface folds and villi.

Key words: Phagocytosis, Neutrophil, Membrane Tension, Cell mechanics

Introduction

Phagocytosis is a key capability through which the neutrophil fulfills its role as foot-soldier of the immune system. Although considerable effort has been devoted to elucidating the biochemical signaling pathways that control this process (e.g. May and Machesky, 2001; García-García and Rosales, 2002), the mechanical implementation of phagocytosis has received less attention, in the neutrophil or other cell types [notable exceptions include (Evans et al., 1993; Simon and Schmid-Schönbein, 1988)].

A major obstacle to a thorough analysis of the mechanics of phagocytosis is that almost all experimental data available in the literature pertain to phagocytosis by spread cells. By contrast, the work presented in this paper employs the simplest configuration possible: an initially spherical isolated cell that phagocytoses an opsonized sphere. This has the advantage of geometric simplicity because of formal two-dimensional cylindrical symmetry (around the axis joining the centers of the two spheres). It also avoids the constraints on volume and surface area imposed by adhesion to a substratum. Although such conditions may not be typical of in vivo behavior since activated neutrophils tend to spread and adhere, they have the advantage of stripping the phagocytic process down to its most elementary manifestation, one that is potentially more amenable to modeling and understanding.

Since the creation of a phagosome can require a considerable increase in surface area, an important element of the mechanics of phagocytosis is the behavior of the cortical tension. Tension is both a diagnostic probe and a constraining factor of the transformation that allows a neutrophil to engulf its prey. On one hand, stretching of the surface area of the neutrophil is associated with increases in cortical tension that can be measured (e.g. Needham and Hochmuth, 1992). On the other hand, cortical tension opposes and can even prevent the expansion of surface area needed to envelop the phagocytic target (Simon and Schmid-Schönbein, 1988).

In this paper we study the time-dependent response of the cortical tension of the neutrophil during phagocytosis. We compare the behavior of the tension in this active, self-driven process with the behavior of the tension during a passive, externally driven deformation in which the neutrophil is aspirated by a micropipette. We show that the neutrophil has the ability to modulate its cortical tension depending on the circumstances of the deformation, thus either enabling or resisting further extension of its surface area. We suggest that this is indicative of active management of spare surface membrane availability geared towards facilitating phagocytosis and opposing passive deformation.

Materials and Methods

Geometrical relations

We assume that the cellular volume $V_0=4/3\pi R_0^3$ remains constant through our experiments (inspection of the data shows that this is the case). In micropipette aspiration experiments a cellular appendage of length L_p protrudes in the pipette (Fig. 1). Relating the cell area A to the length L_p leads to rather complicated mathematical expressions. Moreover, measurements of L_p directly from the microscope images have significant uncertainty in the exact location of the tip of the cell projection into the micropipette because the tip is not always sharply delineated and its apparent location depends on the position of the

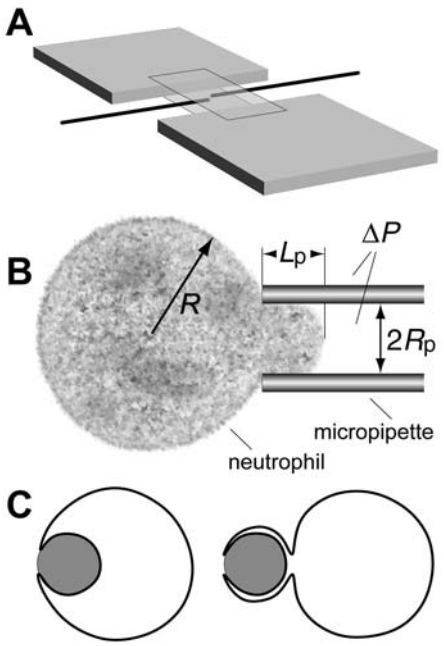

Fig. 1. (A) Layout of the experimental chamber with micropipette access from each side. (B) Measurement of the surface tension by a law of Laplace method. (C) Two geometries of phagocytosis.

image plane. It is therefore for convenience and without real loss of accuracy that we use the following approximate relation:

$$A = 4\pi R^2 + 2\pi R_p[L_p - (R_0 - \sqrt{R_0^2 - R_p^2})] , \quad (1)$$

where the radius R of the body of the cell outside the pipette is related to L_p through the constant volume relation:

$$R = \left(\frac{3}{4\pi} (V_0 - [L_p - (R_0 - \pi\sqrt{R_0^2 - R_p^2})] R_p^2) \right)^{1/3} . \quad (2)$$

The correction to L_p in brackets comes from the natural protrusion of a spherical undeformed cell into the pipette.

In phagocytosis experiments, the configuration after engulfment is typically intermediate between the two geometries depicted in Fig. 1. What we have used for the cell surface area is the average between the two:

$$A = \frac{1}{2} (4\pi[(R_0^3 + R_p^3)^{2/3} + R_p^2] + 4\pi[R_0^2 + 2R_p^2]) . \quad (3)$$

Such an approximation is coarse, but the difficulty in determining the exact geometric configuration due to uncertainties on what is happening outside the image plane as well as the occasional thinness of the lamellipod that surrounds the bead, make a more sophisticated analysis pointless.

Bead preparation

Unmodified polystyrene beads (Polysciences, Warrington, PA; nominal bead diameters 2 μm, 3 μm, 4.5 μm, 6 μm, and 10 μm) were incubated overnight at 4°C with 10 mg/ml bovine serum albumin (BSA) dissolved in phosphate buffered saline (PBS). The beads were then centrifuged and washed with PBS (without BSA) three times and then incubated for 1 hour at room temperature with polyclonal rabbit anti-BSA antibody (ICN Biomedicals, Aurora, OH). The beads were then centrifuged once more and resuspended in PBS before storage at 4°C. The sustained presence of rabbit-Ig coating on the beads over several weeks was confirmed by Fc-targeted fluorescence labeling (FITC-conjugated mouse mAb vs γ-chain Rabbit Ig; Sigma, St Louis, MO).

On days of experiments, small amounts of rabbit-Ig-coated beads were retrieved, sonicated, and washed and spun once in PBS. Volume amounts introduced in the experimental chamber were of the order of 1 to 2 μl.

Cell and chamber preparation

A microscope chamber with two open sides that provided simultaneous access for two pipettes facing each other was made from polycarbonate. Microscope coverslips were cut in two, and the two halves were sandwiched to the chamber base with vacuum grease as shown in Fig. 1. The small vertical distance between the cover glasses (2 mm) created sufficient capillary force to retain the buffer in the chamber.

On days of experiments, a drop of whole blood was obtained by finger prick and immediately suspended in heparinized calcium and magnesium-free Hanks' balanced salt solution (HBSS; Sigma, St Louis, MO). A volume amount of the order of 1 to 2 μl was then introduced in the experimental chamber and neutrophils selected visually among the backround erythrocytes. The chamber medium consisted of heparinized HBSS (with Ca and Mg; Sigma) with 10% autologous plasma.

Micromanipulation

Micropipettes were made from 1 mm (OD) borosilicate glass-tube capillaries (Kimble Glass, Vineland, NJ) that were pulled in a pipette puller (David Kopf Instruments, Tujunga, CA) to tip diameters in the range of 2 to 3 μm (ID). Computer-controlled, motorized three-axis translation stages (Newport Corp., Irvine, CA) allowed for coarse pipette positioning and micromanipulation. The pipettes were connected to water reservoirs that could be translated vertically to apply precise suction pressures. Alternatively, the desired pressures could be set quickly by evacuation of the air volume enclosed above the water reservoirs using syringes. In both cases, precalibrated transducers (Validyne Engineering, Northridge, CA) reported the instantaneous value of the pipette-aspiration pressure to an LCD display and to the computer with a resolution of 0.1 mm H_2O (~1 Pa).

The experiments were observed with an Axiovert inverted microscope (Carl Zeiss Microimaging, Thornwood, NY) using a 63× objective and brightfield illumination. A cooled 12-bit video camera (SensiCam, The Cooke Corp., Auburn Hills, MI) and a dedicated digitizer enabled us to monitor the experiments on the computer screen (at 30 fps), while simultaneously saving images to hard disk (up to 10 fps) using custom-written software. The SensiCam was attached to a microscope camera port via a 4× ZEISS adapter, giving video images with a final magnification of 38 nm/pixel.

A suitable neutrophil was picked up in the main micropipette at a low initial holding pressure ΔP that produced a small projection length L_p (see Fig. 1 for notation). In phagocytosis experiments, a second pipette was used to pick up a test bead and bring it into brief contact with the neutrophil. Bead-neutrophil adhesion was almost always immediate, in which case the test bead was released from its holding pipette.

Measurement of the cortical tension

The law of Laplace method is used (Evans and Yeung, 1989) to determine the cortical tension (γ) of a partially aspirated neutrophil. The basic idea is that the critical pressure difference ΔP at which the cell maintains an appendage of stationary length in an aspirating micropipette is related to the tension through the expression:

$$\gamma = \frac{R_p \Delta P}{2(1 - R_p/R)} , \quad (4)$$

where the symbols are as defined in Fig. 1. To monitor the membrane tension during phagocytosis, the aspiration pressure was continually adjusted in such a way that the projection length remained nearly constant.

Cortical tension

Our starting point is a previously proposed quantitative model that relates the neutrophil cortical tension to changes in apparent cellular area. This model was found to account for the dynamics of cell aspiration into a micropipette and for tension behavior during the formation of an isolated pseudopod following activation with fMLP (Herant et al., 2003). One objective of this work is to ascertain how far this model is applicable in the context of phagocytosis. The main properties of this model are that (1) gradients of cortical tension quickly equilibrate around the cell surface so that the tension is close to uniform over the cell, (2) cortical tension in steady state is determined through a constitutive law by the apparent cell surface area relative to its undeformed (spherical) area, and (3) that cortical tension during dynamical transformation is determined by the cell area and its rate of change.

Cellular deformation changes the apparent cell surface area A which is the macroscopic surface area of the cell as seen by light microscopy (we include in A the area of the nascent phagosome). By contrast, we label A_μ the true microscopic surface area of membrane that includes the multitude of folds and villi observable by electron microscopy (e.g. Needham and Hochmuth, 1992) but hidden to optical microscopy. Those wrinkles constitute a membrane reserve available for cellular deformation that allow A to vary despite membrane inextensibility. One should note, however, that A_μ may also vary due to insertion of new membrane from intracellular vesicular stores. Prior work has shown that the maximum plasma membrane area that is rapidly available (time scale of less than a minute, presumably without vesicle recruitment and simply from wrinkle unfurling) is $\sim 2.1A_0$, where A_0 is the initial apparent area of the spherical neutrophil. At longer time scales or during phagocytosis, this becomes 2.5 to $3A_0$, presumably due to the ability to recruit vesicular membrane (Schmid-Schönbein et al., 1980; Simon and Schmid-Schönbein, 1988; Evans and Yeung, 1989; Ting-Beall et al., 1993). Let the surface tension of the membrane be γ. It is convenient to split γ into two components:

$$\gamma = \gamma_{el} + \gamma_{vis} . \quad (5)$$

The term γ_{el} is the cortical tension under static conditions and γ_{vis} is the additional tension when A is rapidly increasing (unfurling of membrane folds).

The elastic contribution to the cortical tension is modeled by a simple linear function:

$$\gamma_{el} = \gamma_0 + k\frac{A-A_0}{A_0} , \quad (6)$$

where k is the elastic expansion modulus, γ_0 is the baseline surface tension when the cell is spherical. Herant et al. used γ_0=0.025 mN m^{-1} and k=0 based on aspiration and pseudopod protrusion studies (Herant et al., 2003).

The viscous resistance to area expansion is probably due to the irreversible (on short timescales) work of breaking the bonds that hold wrinkles of spare membrane together. It requires more force to convert wrinkles into 'covering membrane' if these bonds have to be broken quickly. The viscous contribution to the surface tension is modeled by a simple linear constitutive relation:

$$\gamma_{vis} = \begin{cases} 0 & \text{if } \frac{dA}{dt} \le 0 \text{ or } A \le A(1+\varepsilon) \\ \nu\frac{dA/dt}{A} & \text{if } \frac{dA}{dt} > 0 \text{ and } A > A(1+\varepsilon) . \end{cases} \quad (7)$$

Here the coefficient ν is a surface viscosity that is only operative for positive area dilation. We further introduce a viscous slack ε which is envisioned to represent the fraction of the initial cell area that can be taken up before it is necessary to break bonds for further expansion. Herant et al. found ν=75 mN^{-1} s, ε=5% (Herant et al., 2003).

This model leads to a number of expectations for the behavior of the cortical tension during phagocytosis.

(1) For very small beads, and at the beginning of the phagocytosis of larger beads, cortical tension should remain constant because area expansion is below the viscous slack threshold.

(2) For larger beads, there should be a transient increase of cortical tension during the stage of rapid area production to create a phagosome. The tension should return near baseline post-phagocytosis as area expansion ceases.

(3) Post-phagocytosis (steady state) cortical tension should increase with the phagocytosis of larger beads because of higher area expansion.

(4) If a cell is pre-stretched prior to phagocytosis, then the viscous slack will be taken up, and even for the ingestion of a small particle, one should see a transient rise in surface tension.

Results

Passive deformation

Passive aspiration of neutrophils has been studied previously by several groups (e.g. Evans and Yeung, 1989; Tsai et al., 1993; Drury and Dembo, 2001). The main reason to revisit the issue here is to provide a rigorous basis for comparison with the phagocytosis experiments. In particular, prior studies have used buffers without calcium to reduce the probability of neutrophil activation. Considering that our phagocytosis experiments take place in a buffer with calcium [otherwise, we found that bead uptake occurs at a low rate (Ducusin et al., 2003)] we felt it necessary to obtain data on passive cell deformation in the presence of this obviously important ion. Two kinds of experiments were performed: (1) static measurements of the cortical tension at steady state for various increases of cell surface area, and (2) dynamic measurements of the cortical tension under various rates of area expansion during aspiration.

Elastic surface tension

By setting a micropipette aspiration pressure ΔP greater than that corresponding to the resting cortical tension γ_0 of the round cell by Eqn 4, it is possible to determine cortical tension versus surface area. For instance Fig. 2 shows that applying a constant aspiration pressure of 0.4 cm H_2O with a pipette of radius 1.2 μm on a neutrophil of radius 4.1 μm eventually results in a constant dilation in cell macroscopic surface area of 16% (due the partial aspiration of the cell into the micropipette). According to Eqn 4, this corresponds to a cortical tension of 0.033 mN m^{-1} for a 16% area expansion. Results from ~40 cells are shown in Fig. 3. Despite scatter indicating heterogeneity in the population, a few clear trends are observed. First, increases of cortical tension occur even for small area expansions, and, at the level of uncertainty afforded by the data, there is no evidence of a threshold effect for the increase of cortical tension. Second, there is a marked increase in stiffness that takes place at a membrane expansion of 25 to 30%. By inspection of Fig. 3, it appears that both the low expansion, soft regime and the high expansion, stiff regime are

approximately linear. A least square fit for area expansions less than 25% yields

$$\gamma = 0.010 + 0.16\,\frac{\Delta A}{A_0}\ \mathrm{mN\,m^{-1}}, \qquad (8)$$

while a least square fit for area expansion greater than 30% yields

$$\gamma = -0.50 + 2.14\,\frac{\Delta A}{A_0}\ \mathrm{mN\,m^{-1}}. \qquad (9)$$

Combining Eqns 8 and 9 gives the critical area expansion at the transition from the soft to stiff regime which is 26%.

Prior models by Herant et al. used $\gamma = \gamma_0 = 0.025$ mN m^{-1} (k=0) for area expansions up to ~20% (Herant et al., 2003), which is consistent with current data if one averages the tension between 0 and 20% expansion.

Viscous surface tension

A previous study (Herant et al., 2003) showed that the major determinant of the dynamics of neutrophil aspiration in micropipettes is the viscous surface tension generated during dynamical expansion of cell surface area (see also Drury and Dembo, 2001). For small diameter micropipettes, i.e. $R_p \ll R_0$ (as is the case here), the surface viscosity completely dominates cytoplasmic viscosity as the primary dissipating force resisting aspiration. In aspiration experiments, the dependence of cell projection length L_p aspirated into the micropipette versus time has a characteristic pattern consisting of an initial jump followed by a steady entry speed. This has been interpreted by Herant et al. as indicative of membrane slack that has to be taken up during the initial jump before viscous surface tension due to area expansion kicks in (Herant et al., 2003).

A typical aspiration curve is given in Fig. 2, where the area expansion is obtained per Eqn 1. Examination of 23 cell aspiration curves yields a distribution of slack areas given by the location of the shoulder in the aspiration curve, and surface viscosity given by the slope of the linear portion (at low area expansion ~10-20%) of the aspiration curve as a function of aspiration pressure. The histograms in Fig. 4 show a mean slack parameter of ε=5.7±0.3% (standard deviation 1.5%) and a mean surface viscosity of ν=72±8 mN m^{-1} s (standard deviation 41 mN m^{-1} s) for passive aspiration.

These values are in excellent agreement with those derived by Herant et al. for models of neutrophil aspiration using a different dataset (ε=5%, ν=75 mN m^{-1} s) (Herant et al., 2003). Thus, the presence of calcium in the incubating medium does not appear to significantly impact the dynamics of the neutrophil during passive aspiration.

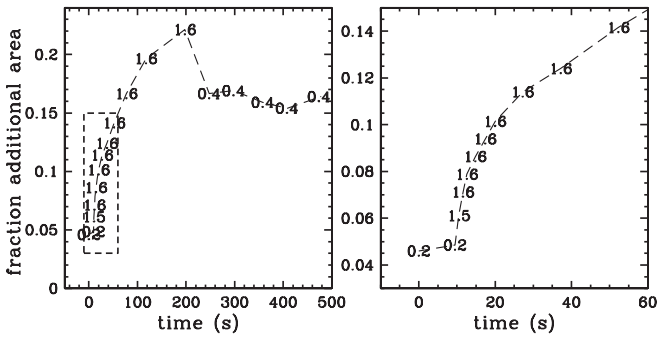

Fig. 2. Curves showing macroscopic cell area dilation over time during micropipette aspiration (numbers indicate aspiration pressure in cm H_2O). (Left) Steady state area expansion under a fixed aspiration pressure. (Right) Initial jump followed by steady expansion (detail of left curve). Neutrophil radius was 4.1 μm and micropipette radius was 1.2 μm.

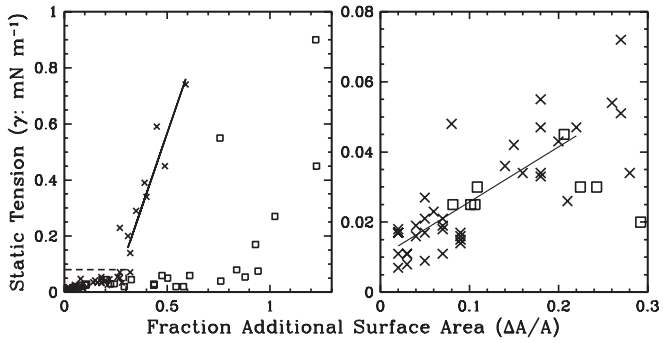

Fig. 3. Cortical tension versus area expansion in neutrophils post partial aspiration (×) and in neutrophils post-phagocytosis (□). Each data point represents a different neutrophil. The right panel shows in detail the boxed area in the left panel. Straight lines are fits to the aspiration data at less than 25% expansion (right) and more than 30% expansion (left; see Eqns 8 and 9).

Phagocytosis

We studied the time course of neutrophil phagocytosis of Ig-coated beads of different radii (Table 1). Bead presentation always resulted in nearly immediate (within seconds) adhesion

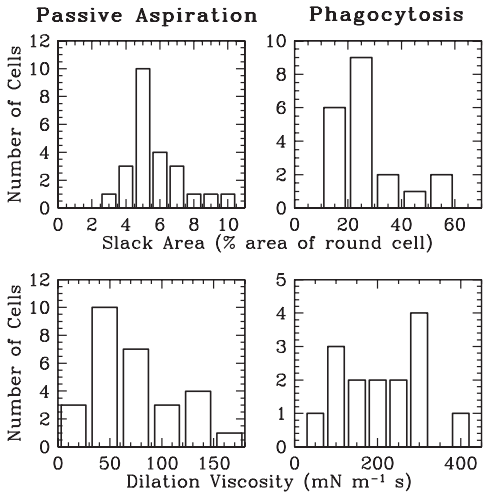

Fig. 4. (Top left) Histogram of percentage area of slack membrane taken up before viscous surface tension occurs under passive aspiration (24 cells, mean 5.7%, s.d. 1.5%). (Top right) As for top left but in phagocytosis (20 cells, mean 27%, s.d. 11%). (Bottom left) Histogram of the magnitude of the surface viscosity under passive aspiration (28 cells, mean 72 mN m^{-1} s, s.d. 41 mN m^{-1} s). (Bottom right) As for bottom left but in phagocytosis (15 cells, mean 200 mN m^{-1} s, s.d. 100 mN m^{-1} s).

Table 1. Number of phagocytoses (N) successfully observed and analyzed for each class of beads

Bead diameter	N
2 μm	5
3 μm	6
4.5 μm	8
6 μm	7
11 μm	6
3 μm ×2	3
3 μm*	7

*Beads phagocytosed by pre-streched neutrophils.

to the cell surface. Thereafter, phagocytosis began after various delay times (seconds, minutes, fractions of an hour) and sometimes it never occurred at all. In general, the initiation of phagocytosis was more rapid for larger beads. Phagocytosis of beads of radius >3 μm began immediately after contact and adhesion. Phagocytosis of beads of radius 2-3 μm often took a few minutes to start. For the smallest beads (radius ~1.2 μm), phagocytosis occurred within 15 minutes of adhesion only about 25% of the time, and we were often unable to observe phagocytosis at all. This dependence of phagocytic activity on the size of the phagocytic target is in agreement with previous reports (Koval et al., 1998; Volle et al., 2000).

In our experiments, the beginning of phagocytosis is not a subtle event: once a rim of cytoplasm begins to envelop the bead, there is no reversal and no apparent pause greater than a minute or so until engulfment is complete. This seems to indicate that once a threshold signal is reached, the cell is committed to the phagocytic process. Even when the bead is obviously too large to be enclosed, we never observe the neutrophil 'giving up' and rounding up again.

Images representative of phagocytosis of beads of various radii are shown in Fig. 5. For each phagocytosis, the percentage of the bead engulfed was estimated as a function of time by visual inspection of the images (Fig. 6). Such estimates are 'best guesses' as it is often difficult to tell exactly how far the rim of the phagocytic cup has progressed around the bead.

The time course of the cortical tension was measured by continually adjusting the aspiration pressure of the holding pipette with the goal of keeping the length of the aspirated portion of the neutrophil stationary. Images were audited post collection and only time points that showed no motion of the projection, relative to the bracketing before and after frames, were used to determine the tension. Note that the engulfment and tension versus time curves presented in Fig. 6 were found to be typical of the behavior observed for other phagocytoses not shown here.

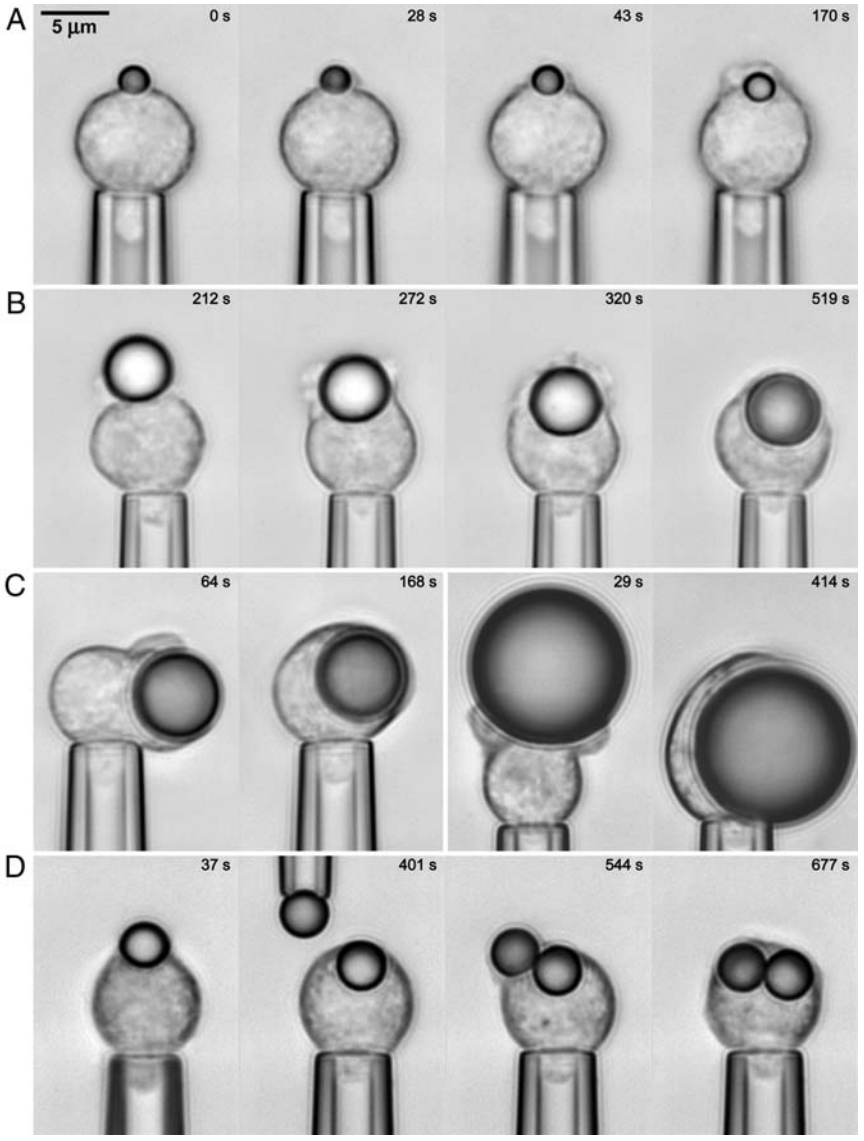

Fig. 5. (A) Phagocytosis of a bead of radius 1.1 μm by a neutrophil of radius 4.2 μm. (B) phagocytosis of a bead of radius 2.3 μm by a neutrophil of radius 4.2 μm. (C) left, phagocytosis of a bead of radius 3.3 μm by a neutrophil of radius 4.5 μm; right, attempted phagocytosis of a bead of radius 5.5 μm by a neutrophil of radius 4.4 μm. (D) Sequential phagocytosis of two beads of radii 1.6 and 1.7 μm by a neutrophil of radius 4.3 μm.

Elastic surface tension

In the course of our phagocytosis experiments, neutrophils begin from a spherical steady-state configuration and eventually return to a roughly ellipsoidal steady-state configuration that includes an internal phagosome (except of course when the bead is too large to be taken up). In the interval, a considerable increase of macroscopic cell area A occurs, leading to a significant viscous contribution to the cortical tension (Fig. 6). However, after return to equilibrium when A is no longer varying, the tension decreases back to a value that is determined by the elastic static tension γ_{el}.

Fig. 3 shows the final cortical tension of

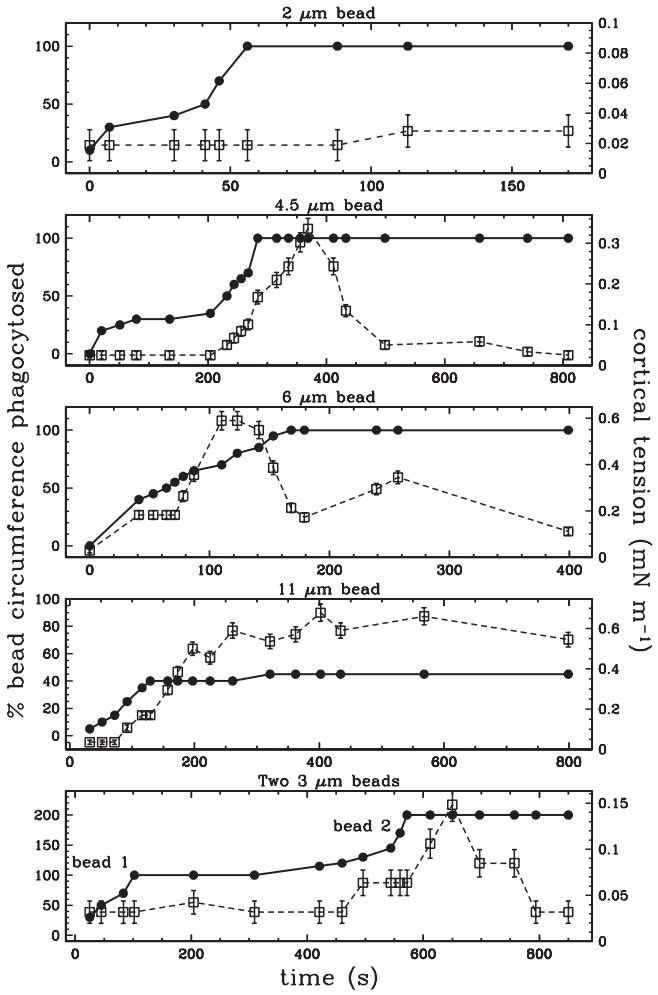

Fig. 6. Percentage of bead circumference phagocytosed (●) and neutrophil cortical tension (□) versus time for cases shown in Fig. 5.

the post-phagocytosis neutrophil versus the expenditure of surface area during phagocytosis as given by Eqn 3. Cortical tension remains low for expansions up to about 80% of surface area but then sharply increases in a way that appears similar to the rise of tension seen in passive aspiration when expansion reaches 30%.

Viscous surface tension

The rapid increase in macroscopic cell surface area that occurs during phagocytosis leads one to expect a large contribution from the viscous component of the surface tension, as defined in Eqn 7. However, simple inspection of the tension curves shows that the phagocytosis of beads of diameter 2 and 3 μm hardly registers in the tension (this was observed in 11/11 phagocytosis events involving small beads). It is only beads of diameter 4 μm and above that show a robust peak in cortical tension during phagocytosis (Fig. 6). As seen in passive aspiration, this is evidence for a threshold of area increase below which no viscous contribution to the surface tension occurs. This is supported by the finding that, on consecutive phagocytoses of two 3 μm beads by the same neutrophil, the first bead does not evoke a response in the tension whereas the second does (Fig. 6, this was observed in 3/3 double-phagocytosis events of 3 μm beads). Presumably this indicates that the membrane slack has been taken up by the first bead.

We have evaluated the membrane slack during phagocytosis in two different ways. From our range of bead and neutrophil radii, we estimate the threshold for onset of viscous surface tension to correspond to the phagocytosis of a 1.8 μm bead radius by a neutrophil of radius 4.3 μm. By using Eqn 3, this corresponds to a slack parameter ε=29%. The strength of this approach is that the tension curves are unambiguous: either there is or there is not a spike during phagocytosis (Fig. 6). Its weakness is that the determination of the threshold relies on very few (~3) phagocytosis tension curves and that, since we know that the cell population is heterogeneous, outliers might skew the result.

For this reason we have also estimated the threshold by noting that the increase of tension seen with larger beads occurs only after a certain amount of bead circumference has been enveloped. These data are given in histogram form in Fig. 4: mean viscous slack is found to be ε=27±3% (standard deviation 11%). Although this measurement is representative of a significant number of cells, it is clouded by the difficulty of precisely determining the extent of a progressing phagocytic cup. Despite this caveat, the agreement with our alternate estimate is reassuring and supportive of its validity.

Finally, we investigated whether the slack is modified by 'pre-stretching' of the neutrophil. For this purpose we studied phagocytosis of small sub-threshold beads by cells that were previously partially aspirated in a micropipette in such a way that the total area expansion would be expected to reach 30% over the spherical configuration. Fig. 7 shows that in this case, the cortical tension does indeed increase during phagocytosis (a rise in cortical tension was observed in 6/7 experiments on phagocytosis of 3 μm beads by pre-stretched neutrophils).

The magnitude of the surface viscosity (Eqn 7) above the slack threshold must be extracted from the data with some care

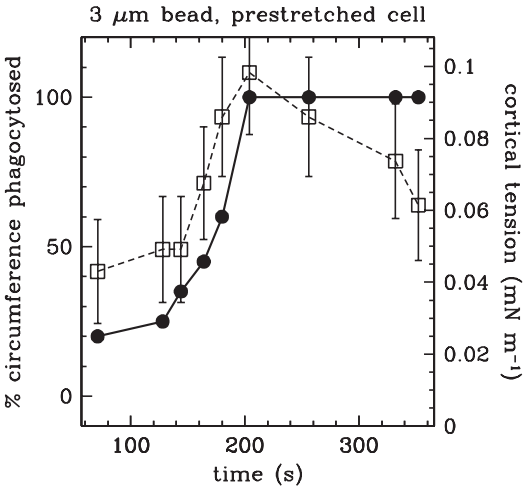

Fig. 7. Phagocytosis of a 1.6 μm radius bead by a 4.2 μm radius neutrophil with a surface area pre-stretched by 14% by aspiration. Percentage of bead circumference phagocytosed (●) and neutrophil cortical tension (□) versus time.

since, in contrast to the aspiration experiments, the time-course of area expansion is not precisely known. By rearranging Eqn 5 and integrating, one can write:

$$\int_{t_s}^{t_f} \gamma_{vis}\, dt = \int_{t_s}^{t_f} \gamma dt - \int_{t_s}^{t_f} \gamma_{el}\, dt\,, \qquad (10)$$

where t_s is the time at which the slack has been taken up during phagocytosis [i.e. when $A = A_{vis} = (1+\varepsilon)\, A_0$)] and t_f is the time after phagocytosis is complete and the tension returns to 'elastic baseline'. The left-hand side term can be computed with the help of Eqn 7:

$$\int_{t_s}^{t_f} \gamma_{vis}\, dt = \int_{t_s}^{t_f} \nu \frac{dA/dt}{A}\, dt = \nu \ln \frac{A_f}{A_{vis}}\,, \qquad (11)$$

where the final area A_f is given by Eqn 3, and $A_{vis} = 1.27\, A_0$ is as determined above. The first term of the right-hand side of Eqn 10 can be directly integrated from the tension data. As for the second term, γ_{el} is considered to be small and is approximated to be linearly varying in time:

$$\gamma_{el} \sim (\gamma_f - \gamma_0) \frac{t - t_s}{t_f - t_s} + \gamma_0\,. \qquad (12)$$

We finally obtain an expression for the surface viscosity:

$$\nu = \frac{\int_{t_s}^{t_f} \gamma dt - \frac{1}{2}(t_f - t_s)(\gamma_f + \gamma_0)}{\ln \frac{A_f}{A_{vis}}}\,. \qquad (13)$$

Surface viscosities were computed for 15 phagocytoses and are given as a histogram in Fig. 4. The mean viscosity was $\nu = 205 \pm 26$ mN m^{-1} s with a large standard deviation of 101 mN m^{-1} s. As discussed below, however, this estimate is fraught with uncertainty related to the increase in total plasma membrane area A_μ due to exocytosis.

Discussion

A compartment picture of surface tension

Excess neutrophil plasma membrane area is stored in folds and villi. During deformations that require an increase in area, membrane is recruited from this reservoir by smoothing out wrinkles, as shown for instance by the disappearance of microvilli in neutrophils during hypotonic swelling (Finger et al., 1996), or by the disappearance of folds in macrophages post-phagocytosis (Petty et al., 1981). It is also accepted that when an area-increasing deforming stress is applied to the cell, surface tension increases and draws membrane out of the wrinkled compartment into the 'covering' compartment (Evans and Kukan, 1984; Schmid-Schönbein et al., 1995; Raucher and Sheetz, 1999).

Following an interpretation previously proposed (Herant et al., 2003), we elaborate on prior work with the following picture of membrane tension (Fig. 8): (1) Wrinkles are stabilized by membrane-cytoskeleton-membrane bonds. (2) Wrinkles see the same surface tension (i.e. are in series). (3) The baseline surface tension is set by the strength of the weakest wrinkle that is at or near thermodynamic equilibrium in the bound/unbound states. (4) When the surface tension increases, the weakest wrinkle is unraveled preferentially thus releasing membrane from the wrinkle compartment to the covering compartment.

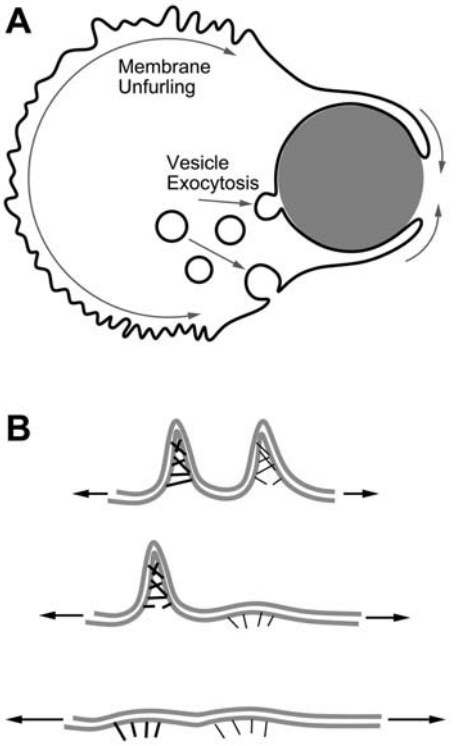

Fig. 8. (A) Sketch of the contributions from unwrinkling of membrane and from vesicular exocytosis to the increasing macroscopic cell surface area during phagocytosis. (B) Sketch of the hierarchical unraveling of membrane wrinkles with stronger cross-links as surface tension increases.

In this two-compartment picture, elastic tension increases with surface area because, as weak wrinkles are recruited, the weakest wrinkle remaining is more tightly bound than previously unraveled wrinkles. Moreover, an additional viscous surface tension component emerges during dynamical expansion of surface area because irreversible breaking of wrinkle-stabilizing bonds dissipates free energy [(e.g. Dembo et al., 1988) for a discussion of this process in the setting of the peeling of a cell off a substrate].

To solidify these concepts let the reaction:

$$A_c \rightleftharpoons A_w \qquad (14)$$

describe the process of conversion of covering membrane to wrinkled membrane and vice versa. Through a law of mass action type of ansatz, we can write:

$$\frac{dA_w}{dt} = -\frac{dA_c}{dt} = k_+ A_c - k_- A_w = k_+ A_c \left(1 - K \frac{A_w}{A_c}\right), \qquad (15)$$

where the ratio $K = k_-/k_+$ is the equilibrium constant of the reaction. One can then write K as a Taylor expansion in γ:

$$K = K_0 + K_0'(\gamma - \gamma_0) + \ldots\,, \qquad (16)$$

where $K_0' > 0$ since we expect the equilibrium (Eqn 14) to shift to the covering compartment with increasing surface tension. Returning to the notation introduced in the Materials and

Methods (Cortical tension section: A_c=A, total membrane area A_μ) we have from membrane conservation A_w= A_μ–A. At steady state, we thus have to first order:

$$\gamma = \gamma_0 + \frac{1}{K_0'}\left(\frac{A}{A_\mu - A} - \frac{A_0}{A_\mu - A_0}\right). \quad (17)$$

This expression shows approximate linearity of the surface tension on expansion for small expansions. It also gives a divergence for the surface tension γ as $A \rightarrow A_\mu$.

Returning to the non-steady state condition, inserting Eqn 16 in Eqn 15 gives:

$$\gamma = \gamma_0 + \frac{1}{K_0' k_+}\frac{1}{(A_\mu - A)}\frac{dA}{dt} + \frac{1}{K_0'}\left(\frac{A}{A_\mu - A} - \frac{A_0}{A_\mu - A_0}\right), \quad (18)$$

where we have made use of the fact that K_0= A_0/(A_μ–A_o). Once again, for small area expansions, one obtains an approximately linear relationship of surface tension with rate of area expansion. Evidently, this is an extremely simple model in which we have hidden the physics of the problem in Eqn 16 but it does provide some justification for postulating the existence of a tension stiffness and viscosity.

We have so far assumed that A_μ remains constant. Although this is probably a good assumption in passive cell deformation, phagocytosis is accompanied by the exocytosis of vesicles, which increases the plasma membrane area (see below). In this sense one could consider a three compartment model of the membrane (covering, wrinkled and vesicular) with the caveat that vesicular membrane conversion to other forms is not directly controlled by surface tension (discussed below).

Our proposed interpretation of the origin of surface tension in neutrophils relies on passive processes. This is a choice of simplicity within a minimal model of cortical tension. Unfortunately, parsimony seldom seems to rule biological systems. It is likely that many additional complexities lurk in the background as embodied by the powerful apparatus of signaling and effector molecular agents present in the neutrophil. For instance, active motor mechanisms of production of cortical tension cannot be excluded and are almost certainly active at some level (if only to repackage spare plasma membrane into folds and villi upon return to a spherical cell shape from a deformed state). We note that in the case of *Dictyostelium*, the finding that certain myosin I mutants have decreased surface tension argues in favour of a role for molecular motors (Dai et al., 1999) (although the cortical tension of *Dictyostelium* is approximately 1 mN m^{-1}, which is more than one order of magnitude larger than that of the neutrophil).

Passive deformation versus phagocytosis

The original model by Herant et al. for neutrophil aspiration and pseudopod protrusion proposed a static surface tension of 0.025 mN m^{-1} independent of expansion, a surface viscosity of 75 mN m^{-1} s, and a viscous slack of 5% (Herant et al., 2003). These quantities were deduced from relatively small expansions (<30%). The extension of this characterization to higher expansions and to phagocytosis is discussed below.

Elastic surface tension

We first consider the steady state data for passive deformation. Combined with the physical picture developed above, the bimodal nature of the behavior of the surface tension with area expansion (Fig. 3) strongly suggests the existence of two classes of wrinkles: one that can be unfurled easily, and one that is more tightly stabilized (Fig. 8B). (An alternative equivalent view is that the bases of wrinkles are loosely bound, while the deeper portions are tightly bound.) As the neutrophil departs from a spherical shape and its surface area increases, membrane is first recruited from weak wrinkles leading to a slow rise in surface tension. After all those wrinkles are unfolded, membrane is recruited from more strongly-bound wrinkles and the surface tension rises steeply. It is interesting to note that the transition from soft to stiff regime occurs at an area expansion of ~25%, which corresponds to the increase of surface area of a neutrophil threading a cylinder of diameter slightly less than 5 μm. This happens to be close to the lower limit of capillary diameters and may not be coincidental.

In contrast to passive deformation through aspiration, phagocytosis does not bring about a significant increase in tension after internalization of the bead, except for large beads requiring more than 80% expansion of surface area. This is probably due to an increase of the microscopic plasma membrane area A_μ through recruitment of membrane stored internally in vesicles. This is not a new concept: exocytosis of vesicles during phagocytosis by neutrophils has been directly observed (Suzaki et al., 1997). Moreover, in the case of macrophages, Petty et al. quantified by electron microscopy the internal stores of membrane brought to the surface during phagocytosis to be about 200% of the macroscopic area of the round cell (Petty et al., 1981). In the same vein, it appears from our data that the neutrophil has an internal reserve of membrane equivalent to ~50% of the macroscopic surface area of the round cell (this is on top of the reserve in the form of folds and villi of the plasma membrane, which is ~100% and thus allows a maximum total area expansion ~150%). This internal reserve can be delivered to the plasma membrane during and after phagocytosis resulting in a return to the initial baseline of the cortical tension as long as the area consumed by the creation of a phagosome does not exceed the reserve. We note that some biochemical agents of this membrane recycling pathway have been identified in macrophages and it has been shown that phagocytosis is impaired when this pathway is disrupted (e.g. Bajno et al., 2000; Niedergang et al., 2003).

Viscous surface tension

The viscous component of the surface tension also behaves significantly differently in aspiration and phagocytosis as attested by the results shown in Fig. 4. We consider the viscous slack first; it is increased from 5% in passive aspiration to 27% in phagocytosis. From a physical standpoint, this slack corresponds to the amount of plasma membrane freely available for expansion of cell surface area without dissipative breaking of wrinkle-stabilizing bonds (Fig. 8). Two potential explanations for this difference come to the fore. Delivery of vesicular membrane to the cell surface by exocytosis may delay the need to unfurl wrinkles to create new surface area. Alternatively, the wrinkles themselves may be loosened by the cell as part of the activation of the phagocytosis pathway through enzymatic activity severing the wrinkle-stabilizing

bonds described by Fig. 8. The behavior of the tension during phagocytosis of a sub-threshold bead by a pre-streched neutrophil answers this question (Fig. 7) since, if exocytosis were responsible for the increased threshold, no increase of surface tension should occur.

Two observations are pertinent. First, the viscous slack in phagocytosis of 27% is remarkably close to the critical expansion of 25% at which the transition from soft to stiff regime occurs in passive deformation; this could be explained if the soft class of wrinkles is the specific target of enzymatic unfurling. Second, this mechanism makes sense from a point of view of functionality. The velcro-like nature of the folds and villi distributed over the entire plasma membrane (Fig. 8) dissipates stress when these are unravelled during expansion brought about by passive deformation, thus shielding the potentially dangerous cargo of cytoplasmic granules. During phagocytosis, however, this property impedes engulfment and formation of a phagosome that demands new area: it is therefore advantageous for the cell to release its 'velcro'-stabilized wrinkles instead of requiring extra mechanical work for the stress-driven opening of membrane folds.

Once viscous slack is taken up, the estimated magnitude of the surface tension viscosity is higher during phagocytosis than during passive deformation (~200 mN m^{-1} s vs ~70 mN m^{-1} s). However, this estimate is highly uncertain since it is influenced by the time course of membrane insertion through exocytosis. On the one hand, insertion of new membrane leads to an overestimate of true expansion in phagocytosis, and therefore to an underestimate of the viscosity. On the other hand, since the area expansion is above 30%, the contribution of the static surface tension may be important, which leads to an overestimate of the viscosity (the fact that occasionally the surface tension remains elevated for some time after completion of the phagosome argues in this direction). Finally, we note that surface viscosity is measured for small expansions (10-20%) in aspiration, whereas the phagocytosis figure represents much larger expansions (>30%). In the first case, the viscosity reflects the peeling apart of weakly bound wrinkles (the loose wrinkle class), whereas in phagocytosis it reflects the unfurling of tightly bound wrinkles at higher area expansions.

We gratefully acknowledge technical assistance from M. Bitensky, T. Yoshida, J. Park, V. Debiase, E. Simons, and D. Zhelev. We gratefully acknowledge material support from E. Evans, M. Bitensky and from our funding sources: Whitaker Biomedical Engineering research grant RG-02-0714 to M.H., NIH grant RO1-GM 61806 to M.D. and NIH grant HL 65333 to E. Evans supporting V.H.

References

Bajno, L., Peng, X.-R., Schreiber, A. D., Moore, H. P., Trimble, W. S. and Grinstein, S. (2000). Focal exocytosis of VAMP3-containing vesicles at sites of phagosome formation. *J. Cell Biol.* **149**, 697-705.

Dai, J., Ting-Beall, H. P., Hochmuth, R. M., Sheetz, M. P. and Titus, M. A. (1999). Myosin I contributes to the generation of resting cortical tension. *Biophys. J.* **77**, 1168-1178.

Dembo, M., Torney, D. C., Saxman, K. and Hammer, D. (1988). The reaction limited kinetics of membrane to surface adhesion and detachment. *Proc. R. Soc. Lond. B.* **234**, 55-83.

Drury, J. L. and Dembo, M. (2001). Aspiration of human neutrophils: effects of shear thinning and cortical dissipation. *Biophys. J.* **81**, 3166-3177.

Ducusin, R. J. T., Uzuka, Y., Satoh, E., Otani, M., Nishimura, M., Tanabe, S. and Sarashina, T. (2003). Effects of extracellular Ca^{2+} on phagocytosis and intracellular Ca^{2+} concentrations in polymorphonuclear leukocytes of postpartum dairy cows. *Res. Vet. Sci.* **75**, 27-32.

Evans, E. and Kukan, B. (1984). Passive material behavior of granulocytes based on large deformation and recovery after deformation tests. *Blood* **64**, 1028-1035.

Evans, E. and Yeung, A. (1989). Apparent viscosity and cortical tension of blood granulocytes determined by micropipet aspiration. *Biophys. J.* **56**, 151-160.

Evans, E., Leung, A. and Zhelev, D. (1993). Synchrony in cell spreading and contraction force as phagocytes engulf large pathogens. *J. Cell Biol.* **122**, 1295-1300.

Finger, E. B., Bruehl, R. E., Bainton, D. F. and Springer, T. A. (1996). A differential role for cell shape in neutrophil tethering and rolling on endothelial selectins under flow. *J. Immunol.* **157**, 5085-5096.

García-García, E. and Rosales, C. (2002). Signal transduction during Fc receptor-mediated phagocytosis. *J. Leuk. Biol.* **72**, 1092-1108.

Herant, M., Marganski, W. A. and Dembo, M. (2003). The mechanics of neutrophils: synthetic modeling of three experiments. *Biophys. J.* **84**, 3389-3413.

Hochmuth, R. M. and Marcus, W. D. (2002). Membrane tethers formed from blood cells with available area and determination of their adhesion energy. *Biophys. J.* **82**, 2964-2969.

Koval, M., Preiter, K., Adles, C., Stahl, P. D. and Steinberg, T. H. (1998). Size of IgG-opsonized particles determines macrophage response during internalization. *Exp. Cell Res.* **242**, 265-273.

May, R. C. and Machesky, L. M. (2001). Phagocytosis and the actin cytoskeleton. *J. Cell Sci.* **114**, 1061-1077.

Needham, D. and Hochmuth, R. M. (1992). A sensitive measure of surface stress in the resting neutrophil. *Biophys. J.* **61**, 1664-1670.

Niedergang, F., Colucci-Guyon, E., Dubois, T., Raposo, G. and Chavrier, P. (2003). ADP ribosylation factor 6 is activated and controls membrane delivery during phagocytosis in macrophages. *J. Cell Biol.* **161**, 1143-1150.

Petty, H. R., Hafeman, D. G. and McConnell, H. M. (1981). Disappearance of macrophage surface folds after antibody-dependent phagocytosis. *J. Cell Biol.* **89**, 223-229.

Raucher, D. and Sheetz, M. P. (1999). Characteristics of a membrane reservoir buffering membrane tension. *Biophys. J.* **77**, 1992-2002.

Schmid-Schönbein, G. W., Shih, Y. Y. and Chien, S. (1980). Morphometry of human leukocytes. *Blood* **56**, 866-875.

Schmid-Schönbein, G. W., Kosawada, T., Skalak, R. and Chien, S. (1995). Membrane model of endothelial cells and leukocytes. a proposal for the origin of a cortical stress. *Biomech. Eng.* **117**, 171-178.

Simon, S. I. and Schmid-Schönbein, G. W. (1988). Biophysical aspects of microsphere engulfment by human neutrophils. *Biophys. J.* **53**, 163-173.

Suzaki, E., Kobayashi, H., Kodama, Y., Masujima, T. and Terakawa, S. (1997). Video-rate dynamics of exocytotic events associated with phagocytosis in neutrophils. *Cell Motil. Cytoskel.* **38**, 215-228.

Ting-Beall, H. P., Needham, D. and Hochmuth, R. M. (1993). Volume and osmotic properties of neutrophils. *Blood* **81**, 2774-2780.

Tsai, M. A., Frank, R. S. and Waugh, R. E. (1993). Passive mechanical behavior of human neutrophils: power-law fluid. *Biophys. J.* **65**, 2078-2088.

Volle, J. M., Tolleshaug, H. and Berg, T. (2000). Phagocytosis and chemiluminescence response of granulocytes to monodisperse latex particles of varying sizes and surface coats. *Inflammation* **24**, 571-582.